

# Contrasting Supersymmetry and Universal Extra Dimensions at Colliders

Marco Battaglia

*Lawrence Berkeley National Laboratory, Berkeley, CA 94720, USA*

Asesh K. Datta

*MCTP, University of Michigan, Ann Arbor, MI 48109-1040, USA*

Albert De Roeck

*CERN, Geneva, Switzerland*

Kyoungchul Kong\*, Konstantin T. Matchev

*Physics Department, University of Florida, Gainesville, FL 32611, USA*

We contrast the experimental signatures of low energy supersymmetry and the model of Universal Extra Dimensions and discuss various methods for their discrimination at hadron and lepton colliders. We study the discovery reach of hadron colliders for level 2 Kaluza-Klein modes, which would indicate the presence of extra dimensions. We also investigate the possibility to differentiate the spins of the superpartners and KK modes by means of the asymmetry method of Barr. We then review the methods for discriminating between the two scenarios at a high energy linear collider such as CLIC. We consider the processes of Kaluza-Klein muon pair production in universal extra dimensions in parallel to smuon pair production in supersymmetry. We find that the angular distributions of the final state muons, the energy spectrum of the radiative return photon and the total cross-section measurement are powerful discriminators between the two models.

## 1. INTRODUCTION

Supersymmetry (SUSY) and Extra Dimensions offer two different paths to a theory of new physics beyond the Standard Model (SM). They both address the hierarchy problem, play a role in a more fundamental theory aimed at unifying the SM with gravity, and offer a candidate particle for dark matter, compatible with present cosmology data. If either supersymmetry or extra dimensions exist at the TeV scale, signals of new physics should be found by the ATLAS and CMS experiments at the Large Hadron Collider (LHC) at CERN. However, as we discuss below in Section 2, the proper interpretation of such discoveries may not be straightforward at the LHC and may require the complementary data from an  $e^+e^-$  collider such as CLIC [1].

A particularly interesting scenario of TeV-size extra dimensions is offered by the so called Universal Extra Dimensions (UED) model, originally proposed in [2], where all SM particles are allowed to freely propagate into the bulk. The case of UED bears interesting analogies to supersymmetry and sometimes has been referred to as “bosonic supersymmetry” [3]. In principle, disentangling UED and supersymmetry appears highly non-trivial at hadron colliders [3, 4]. For each SM particle, both models predict the existence of a partner (or partners) with identical interactions. Unfortunately, the masses of these new particles are model-dependent and cannot be used to unambiguously discriminate between the two theories<sup>1</sup>. Both theories have a good dark matter candidate [6] and the typical collider signatures contain missing energy. One would therefore like to have experimental discriminators which relies on the fundamental distinctions between the two models. In what follows we shall discuss methods for experimental discrimination between SUSY and UED. In Section 2 we discuss the case of hadron colliders [7, 8, 9, 10], while in Section 3 we consider a future high energy  $e^+e^-$  collider [11].

---

\*This talk was given by K. Kong, describing past and ongoing work performed in collaboration with the other authors.

<sup>1</sup>Notice that the recently proposed little Higgs models with  $T$ -parity [5] are reminiscent of UED, and they may also be confused with supersymmetry.

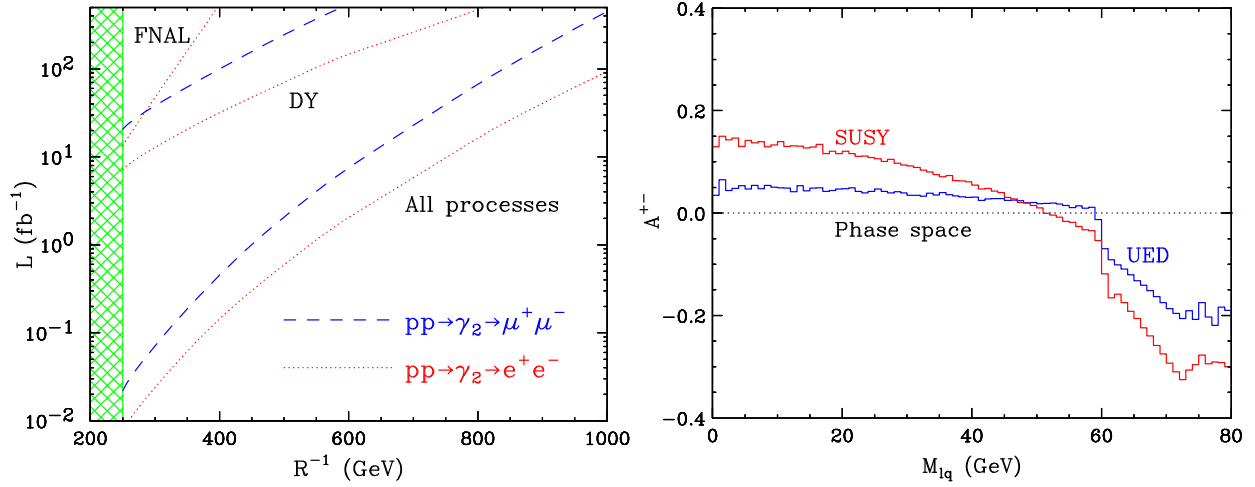


Figure 1: Left:  $5\sigma$  discovery reach of hadron colliders for the level 2 Kaluza-Klein mode  $\gamma_2$  of the photon. The dashed (dotted) lines are for dimuon (dielectron) final states. The lines labelled “DY” only include direct  $\gamma_2$  production in Drell-Yan processes, while the lower set of lines (labelled “All processes”) includes indirect  $\gamma_2$  production from the decays of other level 2 KK modes. For the Tevatron (FNAL) we only show the dielectron reach, including both direct and indirect production. Right: The charge asymmetry defined in Eq. (1) in UED (blue) for  $R^{-1} = 500$  GeV, and in SUSY (red). The SUSY parameters have been chosen to get a matching spectrum. The horizontal dotted line corresponds to the case when all spin correlations are neglected and particles decay according to pure phase space.

## 2. SUSY-UED DISCRIMINATION AT HADRON COLLIDERS

### 2.1. Discovery of the KK tower

One of the characteristic features of UED is the presence of a whole tower of Kaluza-Klein (KK) partners, labelled by their KK level  $n$ . In contrast,  $N = 1$  supersymmetry predicts a single superpartner for each SM particle. One might therefore hope to discover the higher KK modes of UED and thus prove the existence of extra dimensions. However, there are two significant challenges along this route. First, the masses of the higher KK modes are (roughly) integer multiples of the masses of the  $n = 1$  KK partners, and as a result their production cross-sections are kinematically suppressed. Second, the  $n = 2$  KK particles predominantly decay to  $n = 1$  KK modes, which amounts to a small correction to the inclusive production of  $n = 1$  KK particles. Just as in the case of SUSY, because of the unknown momentum carried away by the dark matter candidate at the end of the decay chain, one is unable to reconstruct individual KK resonances. The only exceptions are the level 2 KK gauge bosons, which may appear as high mass dijet or dilepton resonances, when they decay directly to SM fermions through loop suppressed couplings [12].

We studied the prospects for observing the inclusive production of level 2 gauge bosons in UED at the Tevatron and the LHC [7, 8, 9, 10]. We concentrate on the case of  $Z_2$  and  $\gamma_2$  (the level 2 KK partners of the  $Z$ -boson and the photon, correspondingly), which give clean dilepton signatures. (In contrast, the discovery of the level 2 KK gluon  $g_2$  in a dijet channel appears very challenging.) In the left panel of Fig. 1 we show the  $5\sigma$  discovery reach of the Tevatron and the LHC for  $\gamma_2$  [7, 8, 9, 10]. (The reach for  $Z_2$  is very similar.) We studied both dielectron and dimuon final states, and we plot the required total integrated luminosity in  $\text{fb}^{-1}$  as a function of the inverse size of the extra dimension  $R^{-1}$ . We see that already with  $10 \text{ fb}^{-1}$  of data (one year of low-luminosity running) the LHC will be able to cover all of the cosmologically preferred parameter space of the UED model [6]. We also see that, just like in supersymmetry, there is a significant improvement of the reach once one considers indirect production of the  $\gamma_2$  KK particle, due to  $n = 2$  KK quark decays. Unfortunately, even if the  $\gamma_2$  and  $Z_2$  are discovered, they may still be misinterpreted as ordinary  $Z'$  gauge bosons in extended supersymmetric models. It is therefore necessary to get an independent confirmation of the discovery of an extra dimension by other means.

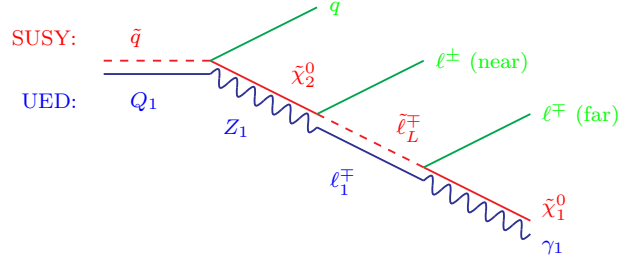


Figure 2: Twin diagrams in SUSY and UED. The upper (red) line corresponds to the cascade decay  $\tilde{q} \rightarrow q\tilde{\chi}_2^0 \rightarrow q\ell^\pm\tilde{\ell}_L^\mp \rightarrow q\ell^\pm\ell^-\tilde{\chi}_1^0$  in SUSY. The lower (blue) line corresponds to the cascade decay  $Q_1 \rightarrow qZ_1 \rightarrow q\ell^\pm\ell_1^\mp \rightarrow q\ell^\pm\ell^-\gamma_1$  in UED. In either case the observable final state is the same:  $q\ell^+\ell^-\cancel{E}_T$ .

## 2.2. Spin determinations

The second fundamental distinction between UED and supersymmetry is reflected in the properties of the individual particles: the KK partners have identical spin quantum numbers as their SM counterparts, while the spins of the superpartners differ by 1/2 unit. However, spin determinations appear to be difficult at the LHC (or at hadron colliders in general), where the center of mass energy in each event is unknown. In addition, the momenta of the two dark matter candidates in the event are also unknown. Recently it has been suggested that a charge asymmetry in the lepton-jet invariant mass distributions from a particular cascade, can be used to discriminate SUSY from the case of pure phase space decays [13] and is an indirect indication of the superparticle spins. It is therefore natural to ask whether this method can be extended to the case of SUSY versus UED discrimination.

To answer this question, we first choose a study point in UED with  $R^{-1} = 500$  GeV. Then we adjust the relevant MSSM parameters until we get a matching spectrum. Following [13], we concentrate on the cascade decay  $\tilde{q} \rightarrow q\tilde{\chi}_2^0 \rightarrow q\ell^\pm\tilde{\ell}_L^\mp \rightarrow q\ell^+\ell^-\tilde{\chi}_1^0$  in SUSY and the analogous decay chain  $Q_1 \rightarrow qZ_1 \rightarrow q\ell^\pm\ell_1^\mp \rightarrow q\ell^+\ell^-\gamma_1$  in UED [9, 10]. Both of these processes are illustrated in Fig. 2.

We then construct the charge asymmetry [13]

$$A^{+-} = \frac{\sigma(q\ell^+) - \sigma(q\ell^-)}{\sigma(q\ell^+) + \sigma(q\ell^-)}, \quad (1)$$

where  $q$  stands for both a quark and an antiquark. The comparison between the case of UED and SUSY [9, 10] is shown in the right panel of Fig. 1. We see that although there is some minor difference in the shape of the asymmetry curves, overall the two cases appear to be very difficult to discriminate unambiguously, especially since the regions near the two ends of the plot, where the deviation is the largest, also happen to suffer from poorest statistics. These results have been recently confirmed in [14].

## 3. SUSY-UED DISCRIMINATION AT LEPTON COLLIDERS

In order to contrast SUSY and UED at lepton colliders, we consider an identical final state in each case:  $\mu^+\mu^-$  and missing energy. This signature may arise either from KK muon production in UED

$$e^+e^- \rightarrow \mu_1^+\mu_1^- \rightarrow \mu^+\mu^-\gamma_1\gamma_1, \quad (2)$$

or from smuon pair production in supersymmetry:

$$e^+e^- \rightarrow \tilde{\mu}^+\tilde{\mu}^- \rightarrow \mu^+\mu^-\tilde{\chi}_1^0\tilde{\chi}_1^0. \quad (3)$$

Again, we choose a UED study point with  $R^{-1} = 500$  GeV, and adjust the SUSY parameters until the two spectra match. For definiteness we fix the collider center-of-mass energy at 3 TeV as is the case of CLIC.

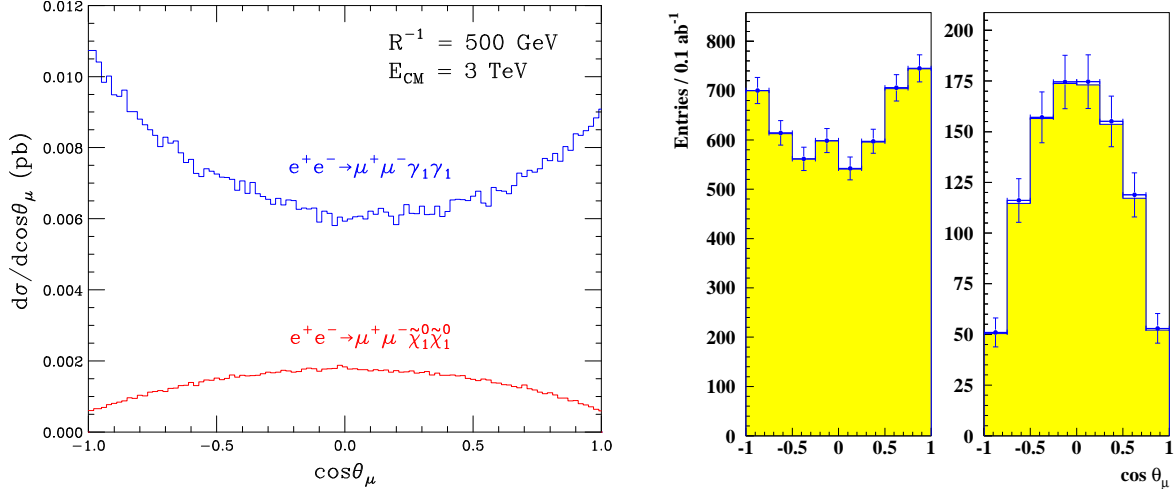


Figure 3: Differential cross-section  $d\sigma/d\cos\theta_\mu$  for UED (blue, top) and supersymmetry (red, bottom) as a function of the muon scattering angle  $\theta_\mu$ . The figure on the left shows the ISR-corrected theoretical prediction. The two figures on the right in addition include the effects of event selection, beamstrahlung and detector resolution and acceptance. The left (right) panel is for the case of UED (supersymmetry). The data points are the combined signal and background events, while the yellow-shaded histogram is the signal only.

### 3.1. Muon angular distributions

In the case of UED, the KK muons are fermions and their angular distribution is given by

$$\left(\frac{d\sigma}{d\cos\theta}\right)_{UED} \sim 1 + \frac{E_{\mu_1}^2 - M_{\mu_1}^2}{E_{\mu_1}^2 + M_{\mu_1}^2} \cos^2\theta \longrightarrow 1 + \cos^2\theta. \quad (4)$$

As the supersymmetric muon partners are scalars, the corresponding angular distribution is

$$\left(\frac{d\sigma}{d\cos\theta}\right)_{SUSY} \sim 1 - \cos^2\theta. \quad (5)$$

Distributions (4) and (5) are sufficiently distinct to discern the two cases. However, the polar angles  $\theta$  of the original KK-muons and smuons are not directly observable and the production polar angles  $\theta_\mu$  of the final state muons are measured instead. But as long as the mass differences  $M_{\mu_1} - M_{\gamma_1}$  and  $M_{\tilde{\mu}} - M_{\tilde{\chi}_1^0}$  respectively remain small, the muon directions are well correlated with those of their parents (see Figure 3a). In Fig. 3b we show the same comparison after detector simulation and including the SM background. The angular distributions are well distinguishable also when accounting for these effects. It is also clear that the total cross-section in each case is very different and provides an alternative discriminator between the models.

### 3.2. Muon energy distributions

The characteristic end-points of the muon energy spectrum are completely determined by the kinematics of the two-body decay and do not depend on the underlying framework (SUSY or UED) as long as the spectra are tuned to be identical. This is illustrated in Fig. 4 (we use the same parameters as in Fig. 3), where we show the ISR-corrected distributions for the muon energy spectra at the generator level (left) and after detector simulation (right).

The lower,  $E_{\min}$ , and upper,  $E_{\max}$ , endpoints of the muon energy spectrum are related to the masses of the particles involved in the decay according to the relation:

$$E_{\max/\min} = \frac{1}{2}M_{\tilde{\mu}} \left(1 - \frac{M_{\tilde{\chi}_1^0}^2}{M_{\tilde{\mu}}^2}\right) \gamma(1 \pm \beta), \quad (6)$$

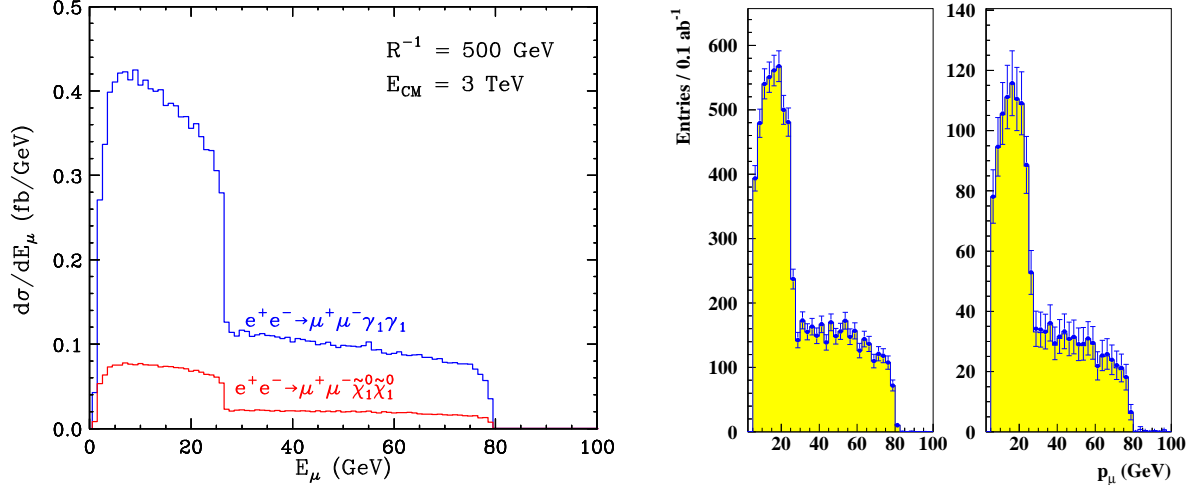


Figure 4: The muon energy spectrum resulting from KK muon production (2) in UED (blue, top curve) and smuon production (3) in supersymmetry (red, bottom curve). The UED and SUSY parameters are chosen as in Fig. 3. The plot on the left shows the ISR-corrected distribution, while that on the right includes in addition the effects of event selection, beamstrahlung and detector resolution and acceptance. The data points are the combined signal and background events, while the yellow-shaded histogram is the signal only.

where  $M_{\tilde{\mu}}$  and  $M_{\tilde{\chi}_1^0}$  are the smuon and LSP masses and  $\gamma = 1/(1 - \beta^2)^{1/2}$  with  $\beta = \sqrt{1 - M_{\tilde{\mu}}^2/E_{beam}^2}$  is the  $\tilde{\mu}$  boost. In the case of the UED the formula is completely analogous with  $M_{\mu_1}$  replacing  $M_{\tilde{\mu}}$  and  $M_{\gamma_1}$  replacing  $M_{\tilde{\chi}_1^0}$ .

Due to the splitting between the  $\tilde{\mu}_L$  and  $\tilde{\mu}_R$  masses in MSSM and that between the  $\mu_1^D$  and  $\mu_1^S$  masses in UED, in Fig. 4 we see the superposition of two box distributions. The left, narrower distribution is due to  $\mu_1^S$  pair production in UED ( $\tilde{\mu}_R$  pair production in supersymmetry). The underlying, much wider box distribution is due to  $\mu_1^D$  pair production in UED ( $\tilde{\mu}_L$  pair production in supersymmetry). The upper edges are well defined, with smearing due to beamstrahlung and, but less importantly, to momentum resolution. Nevertheless, there is sufficient information in this distribution to extract the mass of the  $\gamma_1$  particle, given the values of the  $\mu_1^D$  and  $\mu_1^S$  masses, which in turn can be obtained by a threshold scan.

### 3.3. Radiative return photon

With the  $e^+e^-$  colliding at a fixed center-of-mass energy above the pair production threshold, a significant fraction of the KK muon production will proceed through radiative return. Since this is mediated by  $s$ -channel narrow resonances, a sharp peak in the photon energy spectrum appears whenever one of the mediating  $s$ -channel particles is on-shell. In case of supersymmetry, only  $Z$  and  $\gamma$  particles can mediate smuon pair production and neither of them can be close to being on-shell. On the contrary, an interesting feature of the UED scenario is that  $\mu_1$  production can be mediated by  $Z_2$  and  $\gamma_2$  exchange. Since the decay  $Z_2 \rightarrow \mu_1\mu_1$  is allowed by phase space, there will be a sharp peak in the photon spectrum, due to a radiative return to the  $Z_2$ . The photon peak is at

$$E_\gamma = \frac{1}{2} E_{CM} \left( 1 - \frac{M_{Z_2}^2}{E_{CM}^2} \right). \quad (7)$$

On the other hand,  $M_{\gamma_2} < 2M_{\mu_1}$ , so that the decay  $\gamma_2 \rightarrow \mu_1\mu_1$  is closed, and there is no radiative return to  $\gamma_2$ .

The photon energy spectrum in  $e^+e^- \rightarrow \mu_1^+\mu_1^-\gamma$  for  $R^{-1} = 1350$  GeV,  $\Lambda R = 20$  and  $E_{CM} = 3$  TeV is shown in Fig. 5. On the left we show the ISR-corrected theoretical prediction from CompHEP [15] while the result on the right in addition includes detector and beam effects. It is clear that the peak cannot be missed.

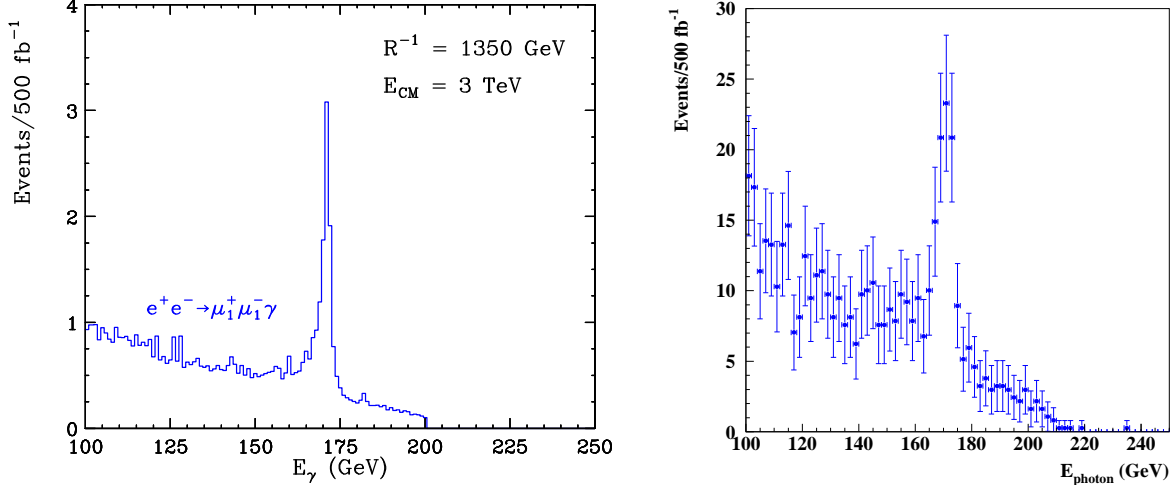


Figure 5: Photon energy spectrum in  $e^+e^- \rightarrow \mu_1^+ \mu_1^- \gamma$  for  $R^{-1} = 1350$  GeV,  $\Lambda R = 20$  and  $E_{CM} = 3$  TeV before (left) and after (right) detector simulation. The acceptance cuts are  $E_\gamma > 10$  GeV and  $1 < \theta_\gamma < 179^\circ$ . The mass of the  $Z_2$  resonance is 2825 GeV.

## Acknowledgments

AD is supported by the US DoE and the Michigan Center for Theoretical Physics. The work of KK and KM is supported in part by a US DoE Outstanding Junior Investigator award under grant DE-FG02-97ER41209.

## References

- [1] The CLIC Study Group, (G. Guignard ed.), CERN-2000-008; C. P. W. Group *et al.*, arXiv:hep-ph/0412251.
- [2] T. Appelquist, H. C. Cheng and B. A. Dobrescu, Phys. Rev. D **64**, 035002 (2001) [arXiv:hep-ph/0012100].
- [3] H. C. Cheng, K. T. Matchev and M. Schmaltz, Phys. Rev. D **66**, 056006 (2002) [arXiv:hep-ph/0205314].
- [4] T. G. Rizzo, Phys. Rev. D **64**, 095010 (2001) [arXiv:hep-ph/0106336]; C. Macesanu, C. D. McMullen and S. Nandi, Phys. Rev. D **66**, 015009 (2002) [arXiv:hep-ph/0201300].
- [5] H. C. Cheng and I. Low, JHEP **0309**, 051 (2003) [arXiv:hep-ph/0308199]; JHEP **0408**, 061 (2004) [arXiv:hep-ph/0405243]; J. Hubisz and P. Meade, Phys. Rev. D **71**, 035016 (2005) [arXiv:hep-ph/0411264].
- [6] G. Servant and T. M. Tait, Nucl. Phys. B **650**, 391 (2003) [arXiv:hep-ph/0206071]; H. C. Cheng, J. L. Feng and K. T. Matchev, Phys. Rev. Lett. **89**, 211301 (2002) [arXiv:hep-ph/0207125].
- [7] K. Matchev, talk given at the “TeV4LHC” workshop, Fermilab, September 17, 2004.
- [8] K. Kong, talk given at the “TeV4LHC” workshop, Brookhaven National Laboratory, February 3, 2005.
- [9] K. Matchev, talks given at the APS meeting, Tampa, FL, April 16 and 17, 2005.
- [10] K. Kong, talk given at the Pheno 2005 Symposium, Madison, WI, May 3, 2005.
- [11] M. Battaglia, A. Datta, A. De Roeck, K. Kong and K. T. Matchev, JHEP **0507**, 033 (2005), [arXiv:hep-ph/0502041].
- [12] H. Georgi, A. K. Grant and G. Hailu, Phys. Lett. B **506**, 207 (2001) [arXiv:hep-ph/0012379]; G. von Gersdorff, N. Irges and M. Quiros, Nucl. Phys. B **635**, 127 (2002) [arXiv:hep-th/0204223]; H. C. Cheng, K. T. Matchev and M. Schmaltz, Phys. Rev. D **66**, 036005 (2002) [arXiv:hep-ph/0204342].
- [13] A. J. Barr, Phys. Lett. B **596**, 205 (2004) [arXiv:hep-ph/0405052].
- [14] J. M. Smillie and B. R. Webber, arXiv:hep-ph/0507170.
- [15] A. Pukhov *et al.*, arXiv:hep-ph/9908288.